An Optimized 3D Inversion Recovery Prepared Fast Spoiled Gradient Recalled Sequence with Multiple Echoes (IR FSPGR ME) for Carotid Plaque Imaging

D. C. Zhu[1], J. K. DeMarco[2], and A. T. Vu[3]

[1]Departments of Psychology and Radiology, Michigan State University, East Lansing, MI, United States, [2]Department of Radiology, Michigan State University, East Lansing, MI, United States, [3]GE Healthcare, Waukesha, WI, United States

Introduction

Intraplaque hemorrhage into the carotid atherosclerotic plaque has been shown to create instability and progression. Moody et al. developed a T_1-weighted magnetization-prepared 3D gradient echo sequence to characterize the hemorrhagic carotid plaque at 1.5T with a good sensitivity and specificity (1). We have also developed a similar optimized 3D inversion recovery prepared fast spoiled gradient recalled sequence (IR FSPGR) on a 3T scanner for carotid plaque imaging and have achieved a good level of success (2). Presented in this paper is a further development of this optimized IR FSPGR, with an inclusion of multiple echo acquisitions. This optimized 3D IR FSPGR with multiple echoes (IR FSPGR ME) maintains the ability of its single-echo technique with respect to blood and fat signal suppression at the carotid region, high-resolution volumetric visualization and hemorrhage detection. In addition, this 3D IR FSPGR ME sequence offers the ability of T_2* mapping, which in turn potentially further characterizes the hemorrhage type (3). This hemorrhage type characterization may provide additional information on plaque vulnerability. Furthermore, image combination from different echoes provides a higher signal to noise ratio (SNR), comparing with the individual echoes as wells as the single-echo IR FSPGR, and thus allows better plaque visualization.

Methods

In this 3D IR FSPGR ME sequence, multiple echoes are acquired after each RF excitation pulse at each slice phase-encoding step. By properly selecting the time of inversion (*TI*) as well as the rest time after the sequence of slice phase encoding steps, the signal from the blood flow can be minimized to reach the maximum contrast between the carotid vessel lumen and the vessel wall. The T_2* was calculated based on the semi-log linear regression of the voxel signal values and the corresponding *TE*s (time of echo). Specifically, $1/T_2^* = -[\ln S_n - \ln S_m)/(TE_n - TE_m)]$, where S_n and S_m are voxel signal intensity at *TE* values of TE_n and TE_m. The weighted-averaged images of the multiple echoes were obtained by $S_{ave} = (S_1 \times (S_1/(S_1+S_2) + S_2 \times (S_2/(S_1+S_2))$, or
$S_{ave} = (S_1 \times (S_1/(S_1+S_2+S_3) + S_2 \times (S_2/(S_1+S_2+S_3) + S_3 \times (S_3/(S_1+S_2+S_3))$ for corresponding two-echo and three-echo IR FSPGR ME sequences, where S_{ave} = signal weighted average, S_1 = signal at TE_1, S_2 = signal at TE_2, S_3 = signal at TE_3. The weighted averaging increases the SNR compared with individual echo as well as emphasizing the signal at the first echo so that the ability of hemorrhage detection is maintained.

Single-echo IR FSPGR, two-echo IR FSPGR ME and three-echo IR FSPGR ME protocols were applied to collect our preliminary data (two patients with known carotid plaque hemorrhage and two healthy adults) on a 3T Signa® HDx MR scanner (GE Healthcare, Waukesha, WI) using a dedicated 4-channel carotid surface coil. For all three protocols, the following parameters were applied: fat saturation, flip angle = 15°, receiver bandwidth = ± 31.25 kHz, field of view = 16 cm, number of slices = 40, slice thickness = 1 mm, matrix size = 256 × 192. Other scanning parameters are shown in Table 1 below.

Table 1. Other Imaging Parameters for IR FSPGR and IR FSPGR ME

	Scan time	1st TE (ms)	2nd TE (ms)	3rd TE (ms)	tr (ms)	Effect TI (ms)	Rest time (ms)	TR (ms)	Number of Excitation
Single-echo IR FSPGR	4 min 23 sec	3.2	None	None	13.2	308	0	572	2
Two-echo IR FSPGR ME	6 min 59 sec	3.3	7.8	None	18.3	421	150	937	2
Three-echo IR FSPGR ME	3 min 44 sec	3.3	7.8	12.2	22.8	520	0	976	1

tr = time of repetition for each phase encoding step, TR = the time of repetition with respect to the non-selective inversion, and
Rest time = the extra rest time after the sequence of slice phase encoding steps.

More traditional quadruple inversion-recovery T_1-weighted (4), double inversion-recovery T_2-weighted (5) and time-of-flight (TOF) images for carotid plaque imaging were also collected to confirms whether the hemorrhagic regions were type I or type II (3).

Results and Discussion

Figure 1 show images from the patient who appeared to have a type I hemorrhage at the right carotid plaque and type II hemorrhage at the left carotid plaque based on the T_1-weighted, T_2-weighted and TOF images (3). The T_2* maps generated from both the two-echo and three-echo IR FSPGR ME sequences show that the type II hemorrhagic region has longer T_2* values than the type I hemorrhagic region. The T_2* values calculated from the three-echo sequence appear more accurate, although conventional T_2* map (with 6 or more echoes) is needed to confirm this observation. 3D IR FSPGR ME technique can potentially be used to further characterize hemorrhage. Despite the shortest scan time, the weighted-averaged image from the three-echo IR FSPGR ME shows better SNR than the longer single-echo IR FSPGR and similar SNR as the longest two-echo IR FSPGR ME protocol (Figure 1). The weighted averaged image has a higher SNR than the images at individual *TE*s as expected. Therefore, weighted averaging of the multiple echoes can be exploited to further improve plaque visualization. We are still investigating an optimized rest time to achieve black blood suppression for the three-echo IR FSPGR ME sequence.

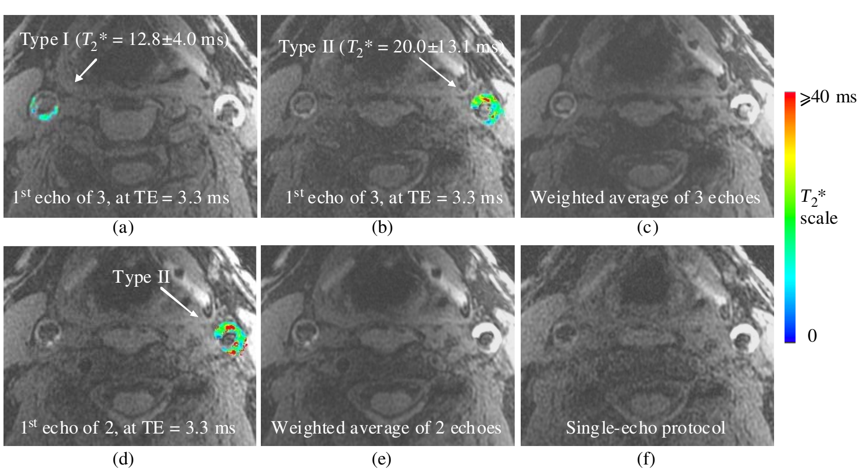

Figure 1. Images are compared between different techniques. Figures (a), (b) and (c) are from three-echo IR FSPGR ME. Figure (d) and (e) are from two-echo IR FSPGR ME. Figure (f) is from single-echo IR FSPGR. The hemorrhagic regions are overlaid with T_2* color maps. The T_2* color scale is shown at the right.

References

1. Moody AR, Murphy RE, Morgan PS, Martel AL, Delay GS, Allder S, MacSweeney ST, Tennant WG, Gladman J, Lowe J, Hunt BJ. Circulation. 2003;107:3047-3052.
2. Zhu DC, DeMarco JK, Ferguson M. International Society for Magnetic Resonance in Medicine, 15th Scientific Meeting and Exhibition, 2007.
3. Saam T, Cai J, Ma L, Cai YQ, Ferguson MS, Polissar NL, Hatsukami TS, Yuan C. Radiology. 2006;240:464-472.
4. Yarnykh VL, Yuan C. Magn Reson Med. 2002;48:899-905.
5. Yarnykh VL, Yuan C. J Magn Reson Imaging. 2003;17:478-483.